American Journal of Engineering Research (AJER)
e-ISSN: 2320-0847 p-ISSN : 2320-0936
Volume-6, Issue-9, pp-288-300
www.ajer.org
Research Paper Open Access

Cellular Vortex Element Modeling Of Multiphase Fluid Flow In Fractured Homogenous 3-D Oil Reservoir

*Oyetunde Adeoye Adeaga[1], Ademola Adebukola Dare[2]
[1] (Department of Mechanical Engineering, Faculty of Engineering, The Ibarapa Polytechnic, Eruwa, Nigeria)
[2](Department of Mechanical Engineering, Faculty of Technology, University of Ibadan, Nigeria)
Corresponding Author: Oyetunde Adeoye Adeaga

Abstract: *Implementation of numerical schemes like finite element, finite volume and finite difference methods in the analysis of subsurface fractured porous media (e.g. oil reservoir) are characterized by grid based solutions and several computer iterations thereby promoting large computer memory usage. Cellular vortex method has relative advantages of avoiding iterations and also providing solutions to moving grids, hence the application of cellular vortex element method to investigate multiphase fluids flow in fractured homogenous oil reservoir. Numerical models for multiphase fluids flow in oil reservoir were developed by the combination of mass conservation principle, Darcy's flow equation, channel-flow theory, equation of state, and continuity equation. Fortran computer program was developed for vorticity equations using convectional algorithms to investigate conditions of reservoir fluids during continuous withdrawals of 0.46×10^{-15} m^3/s (250 bb/d), 0.92×10^{-15} m^3/s (500 bb/d),1.84×10^{-15} m^3/s (1,000 bb/d), 2.30×10^{-15} m^3/s (1,250 bb/d), and 2.76×10^{-15} m^3/s (1,500 bb/d) for 365 days by gravity drainage from a vertical well bore of diameter 0.0762m in a reservoir of dimensions 100×100×225m. For the withdrawals, the mean oil saturations were 0.99±0.01, 0.73±0.19, 0.55±0.05, 0.32 ± 0.038 and 0.01±0.01, while the corresponding mean gas saturations were 0.01±0.02, 0.27 ± 0.09, 0.45± 0.01, 0.6 ±0.04 and 0.99±0.01.Decreasing trends in the oil saturations and corresponding increase in gas saturations were evident.*

Keywords: *Cellular vortex, Darcy, fractured, homogenous, multiphase, oil reservoir, porous media, saturations, transport, vorticity*

Date of Submission: 10-07-2017 Date of acceptance: 23-09-2017

I. INTRODUCTION

Crude oil and natural gas are found in large underground deposits (usually termed reservoirs or pools) in sedimentary basins around the world. The largest oil reservoir in the world (the Arab D limestone in Ghawar in Saudi Arabia) is approximately 230km long and 30km wide and 90m thick [1]. While most commercially exploited minerals and ores exist as solid rocks and have to be physically dug out of the ground, oil and gas exist as fluids underground. They occupy the connected pore space within strata of sedimentary rocks, typically sandstones or carbonates. Oil and gas are extracted by creating pressure gradients within the reservoir that cause the oil and/or gas to flow through the interconnected pores to one or more production wells. The rock formations are typically heterogeneous at all length scales in between, and phenomena at all length scales can have a profound impact on flow, making flow in subsurface reservoirs a true multiscale problem. Observing dynamic fluid behavior and measuring the pertinent parameters of a subsurface reservoir is difficult. Predicting reservoir performance therefore has a large degree of uncertainty attached [2]. Simulation studies are usually performed to quantify this uncertainty. Reservoir simulation is the means by which one uses a numerical model of the geological and petro-physical characteristics of a hydrocarbon reservoir to analyze and predict fluid behavior in the reservoir over time. In its basic form, a reservoir simulation model consists of three parts: (i.) a geological model in the form of a volumetric grid with cell/face properties that describes the given porous rock formation; (ii) a flow model that describes how fluids flow in a porous medium, typically given as a set of partial differential equations expressing conservation of mass or volumes together with appropriate closure relations; and (iii) a well model that describes the flow in and out of the reservoir, including a model for flow within the well bore and any coupling to flow control devices or surface facilities. Reservoir simulation is used for two main purposes: (i) to optimize development plans for new fields; and (ii) assist with operational and investment

decisions. In particular, simulation is used in inverse modeling to integrate static and dynamic (production) data. The role and need for simulation depends greatly depend on the geological setting, the production environment (onshore versus offshore), and field maturity [3]. In any petroleum/oil reservoir, understanding of the subsurface structure is an essential part in respect of growing oil and gas demands in the world. Reservoir characterization and modeling are keys to match the production profile and well planning in the oil field. Now, reservoir computational simulation, in spite of its young age, has found a logical and applicable site in scientific research works [4].

Numerical techniques that are commonly used to investigate fluids dynamics in sub-surface porous media are characterized by mathematical expressions that usually consume useful computer memory, hence reduces processing speed. Black oil reservoirs are important sub-surface porous media in that more than half of the word's energy supply are currently tapped from them. Finite Difference and Finite Element methods that require simultaneous solutions of all grid points are embedded with generation of large matrices, inverses and transposes of the so generated matrices, which eventually exposes the analysis and computations to various errors and hence, occupies useful computer memory in LMS (Large Model Simulation) and these consequently reduce computation speed and enhance resources wastage. Cellular vortex technique has been observed to overcome those lapses on the computer systems. Most existing solution techniques for Reservoir simulation are rigidly grid based (i.e. solutions falls on grid points otherwise no solution exist) but Vortex technique can handle both grid based solution and off -grid based solution(s) and thus can be described as a movable / flexible grid solution method. Existing application of vortex methods were done with or on either surface fluid flow or conduit and flow through pipes which is far different from flow through subsurface media where the flow is overwhelmingly through porous media in which fluid flow measurement is practically impossible. The primary objective of this paper, is to predict future performance of a reservoir and find ways and means of increasing ultimate recovery. The major aim of this article is to establish the use of cellular vortex element technique as an efficient and viable numerical method with a view to standing as another suitable replacement to other existing methods for the analyses and study of the flow of fluids in subsurface porous media like Oil reservoirs. In vortex methods, the fluid volume is broken up into moving particles called vortices or vortons, each with a position and strength. For each step of the vortex method simulation, the influence of every particle on every other particle must be evaluated. This influence depends on the distance and direction between the particles and the strength of the influencing particle, very much like that for universal gravitation. Note that even though only part of space is ever occupied by vortex elements, their influence covers the entire space; there is a velocity that is computable everywhere. As the particles move relative to each other, these velocity influences will change, further changing both the future motion of the particles and the flow everywhere. Even with just three particles, the resulting motion will be chaotic. With hundreds or thousands, their motion is clearly fluid-like [5]. The Vortex element method is a *Langragian* technique as the cellular is, for obtaining solution to engineering problems. It came to being in 1931 with the *Rosenhead* calculation of the Kelvin-Helmholtz instabilities. In 1967, *Batchelor* obtained solutions to the Partial Differential Equation (PDE) thus; [6]

$$\frac{\partial w}{\partial t} = \upsilon\left(\frac{\partial^2 \omega}{\partial x^2} + \frac{\partial^2 \omega}{\partial y^2}\right) + \sigma\left(\frac{\partial \omega}{\partial x} + \frac{\partial \omega}{\partial y}\right) + \xi \qquad (1.0)$$

as $\omega(r,t) = \frac{\Gamma}{4\pi\upsilon t} \exp\left(-\frac{r^2}{4\upsilon t}\right)$

For all $\upsilon \neq 0$ and $\sigma, \xi = 0$

II. FORMULATION OF GOVERNING EQUATIONS

The complete vorticity evolution transport equation for incompressible fluids flow in Laplacian form as presented by [7] is shown in below as

$$\frac{\partial \omega}{\partial t} = -\overbrace{(u.\nabla)\omega}^{Advection} + \underbrace{(\omega.\nabla)u}_{Vortexstreching} - \overbrace{\omega div(u)}^{Dilational} + \underbrace{\frac{1}{\rho^2}(grad\rho \times gradp)}_{Baroclinical}$$

$$+ \overbrace{\frac{\mu}{\rho^2}(grad\rho \times curl\,\omega)}^{External\ forces} - \underbrace{\frac{4\mu}{3\rho^2}[grad\rho \times grad\,(divu)]}_{External\ forces} + \overbrace{\frac{\mu}{\rho}\nabla^2\omega}^{Viscous\ diffusion}$$

$$+ [\nabla \times [\frac{1}{\rho}(-\frac{2}{3}(\nabla.u)(\nabla\mu) + 2(\nabla u).(\nabla\mu) + (\nabla\mu) \times \omega]\ ]$$

Introducing the material derivative, and simplifying the viscous diffusion term for the case of Newtonian, incompressible fluids with constant kinematic viscosity, υ, leads to the common vorticity equations;

$$\frac{D\omega}{Dt}=\frac{\partial\omega}{\partial t}+\overbrace{(u.\nabla)\omega}^{Advection}=\underbrace{(\omega.\nabla)u}_{Vortex\,stre ching}+\underbrace{\frac{1}{\rho^2}(\nabla\rho\times\nabla p)}_{baroclinical}+\overbrace{\Delta\times f_e}^{Body\ Force}+\overbrace{\upsilon\nabla^2\omega}^{Viscous\ diffusion} \tag{2.0}$$

Assumptions made were;
(1)Fully or slightly incompressible reservoir fluids (2) Negligible gravitational body forces (3) Pressure differences or relative movement of boundaries are caused by fluid motion/dynamics (4) Negligible chemical reaction between media and fluid.(5) Permeability is independent of fluid, temperature, pressure and location within the porous stratum (6) Laminar fluid flow, i. e no turbulence.(7) No electro-kinetic effect (no streaming potentials)(8) No Klinkenberge effect (i.e. no wall or boundary slippage).
Therefore, a modified vorticity equation gives;

$$\frac{D\omega}{Dt}=\frac{\partial\omega}{\partial t}+\overbrace{(u.\nabla)\omega}^{Advection}=\underbrace{(\omega.\nabla)u}_{Vortex\ \ streching}+\overbrace{\upsilon\nabla^2\omega}^{Viscous\ diffusion} \tag{3.0}$$

Hence,

$$\frac{\partial\omega}{\partial t}=-\overbrace{(u.\nabla)\omega}^{Advection}+\underbrace{(\omega.\nabla)u}_{Vortexstre ching}+\overbrace{\upsilon\nabla^2\omega}^{Viscous\ diffusion} \tag{4.0}$$

Where, ω is the vorticity and 'r' is the radius.
Starting with an element of the reservoir, the basic equation for oil flow is derived by combining the continuity equation, the Darcy's flow equation, and equation of state and using a balance on the STB (Stock Tank Barrels) of oil; [8]
Mass rate in – Mass rate out = Mass rate of accumulation. Therefore,

Oil phase

$$\frac{\partial}{\partial x}\left(\frac{k_o}{\mu_o B_o}\frac{\partial P}{\partial x}\right)=\frac{\partial}{\partial t}\left(\frac{\phi S_o}{B_o}\right) \tag{5.0}$$

Water Phase

$$\frac{\partial}{\partial x}\left(\frac{k_w}{\mu_w B_w}\frac{\partial P}{\partial x}\right)=\frac{\partial}{\partial t}\left(\phi\frac{S_w}{B_w}\right) \tag{6.0}$$

Gas Phase

The mass balance for the gas phase must include all possible sources of gas. For a linear system we can conveniently that:

$$\frac{\partial}{\partial x}\left[\left(\frac{k_g}{\mu_g B_g}+\frac{R_{so}K_o}{\mu_o B_o}+\frac{R_{sw}K_w}{\mu_w B_w}\right)\frac{\partial P}{\partial x}\right]=\frac{\partial}{\partial t}\left[\phi\left(\frac{S_g}{B_g}+\frac{R_{so}S_o}{B_o}+\frac{R_{sw}S_w}{B_w}\right)\right] \tag{7.0}$$

The generalized multiphase flow equation for the steady-state flow of oil, gas, and water in a porous medium is developed by combining the three single-phase flow equations into one basic equation.

Equation for Oil phase in 1-D

$$A_x\frac{\partial}{\partial x}\left\{\frac{k_o}{\mu_o B_o}\frac{\partial\Phi_o}{\partial x}\right\}+q_o=V_R\frac{\partial}{\partial t}\left(\frac{\phi S_o}{B_o}\right) \tag{8.0}$$

Equation for Water phase in 1-D

$$A_x \frac{\partial}{\partial x}\left\{\frac{k_w}{\mu_w B_w}\frac{\partial \Phi_w}{\partial x}\right\} + q_w = V_R \frac{\partial}{\partial t}\left(\frac{\phi S_w}{B_w}\right) \tag{9.0}$$

Equation for Gas phase in 1-D

$$A_x \frac{\partial}{\partial x}\left\{\frac{k_g}{\mu_g B_g}\frac{\partial \Phi_g}{\partial x} + \frac{R_{so}k_o}{\mu_o B_o}\frac{\partial \Phi_o}{\partial x} + \frac{R_{sw}k_w}{\mu_w B_w}\frac{\partial \Phi_w}{\partial x}\right\} + q_g = V_R \frac{\partial}{\partial t}\left(\phi\left(\frac{S_g}{B_g} + \frac{R_{so}S_o}{B_o} + \frac{R_{sw}S_w}{B_w}\right)\right) \tag{10.0}$$

Complete 1-D multiphase fluid flow gives,

$$A_x\left[\left(M_o\right)\left(1+B_{g/o}R_{so}\right)+\left(M_w\right)\left(1+B_{g/w}R_{Sw}\right)+\left(M_g\right)\right]\frac{\partial^2 P_o}{\partial x^2}+$$

$$A_x\left[B_o\frac{\partial}{\partial x}\left(\frac{M_o}{B_o}\right)+B_w\frac{\partial}{\partial x}\left(\frac{M_w}{B_w}\right)+B_g\left(\frac{\partial}{\partial x}\left(\frac{M_g}{B_g}\right)+\left(\frac{M_w}{B_w}\right)\frac{\partial R_{sw}}{\partial x}+\left(\frac{M_o}{B_o}\right)\frac{\partial R_{so}}{\partial x}\right)\right]\frac{\partial P_o}{\partial x}+$$

$$A_x\left[\left(M_o gh\frac{\partial^2 \rho_o}{\partial x^2}\right)\left(1+B_{g/o}R_{So}\right)+\left(M_w gh\frac{\partial^2 \rho_w}{\partial x^2}\right)\left(1+B_{g/w}R_{Sw}\right)+\left(M_g gh\frac{\partial^2 \rho_g}{\partial x^2}\right)\right]+$$

$$A_x\left[B_g\frac{\partial}{\partial x}\left(\frac{M_g}{B_g}\right)\frac{\partial P_{cg}}{\partial x}-B_w\frac{\partial}{\partial x}\left(\frac{M_w}{B_w}\right)\frac{\partial P_{cw}}{\partial x}+\left(M_g\right)\frac{\partial^2 P_{cg}}{\partial x^2}-\left(M_w\right)\frac{\partial^2 P_{cw}}{\partial x^2}\right]+$$

$$A_x\left[\left(\left(M_g\right)\frac{\partial^2 P_{cg}}{\partial x^2}-\left(M_w\right)\frac{\partial^2 P_{cw}}{\partial x^2}\right)+\left(\left(M_w\right)\left(B_{g/w}\right)\left(\frac{\partial R_{sw}}{\partial x}\right)\frac{\partial P_{cg}}{\partial x}+\left(M_o\right)\left(B_{g/o}\right)\left(\frac{\partial R_{so}}{\partial x}\right)\frac{\partial P_{cg}}{\partial x}\right)\right]$$

$$+\left(B_g q_g + B_w q_w + B_o q_o\right)$$

$$=$$

$$V_R\phi\left[\left(S_o\left(B_{g/o}\right)\left(\frac{\partial R_{so}}{\partial P_o}\right)+S_w\left(B_{g/w}\right)\left(\frac{\partial R_{sw}}{\partial P_o}\right)\right)-\left(\left(\frac{S_o}{B_o}\right)\frac{\partial B_o}{\partial P_o}+\left(\frac{S_w}{B_w}\right)\frac{\partial B_w}{\partial P_o}+\left(\frac{S_g}{B_g}\right)\frac{\partial B_g}{\partial P_o}\right)\right]\frac{\partial P_o}{\partial t} \tag{11.0}$$

Dividing throughout by,

$$V_R\phi\left[\left(S_o\left(B_{g/o}\right)\left(\frac{\partial R_{so}}{\partial P_o}\right)+S_w\left(B_{g/w}\right)\left(\frac{\partial R_{sw}}{\partial P_o}\right)\right)-\left(\left(\frac{S_o}{B_o}\right)\frac{\partial B_o}{\partial P_o}+\left(\frac{S_w}{B_w}\right)\frac{\partial B_w}{\partial P_o}+\left(\frac{S_g}{B_g}\right)\frac{\partial B_g}{\partial P_o}\right)\right]$$

and expressed as

$$\frac{\partial P_o}{\partial t} = \underbrace{\lambda_5\left[\frac{\partial^2 P_o}{\partial x^2}+\frac{\partial^2 P_o}{\partial y^2}+\frac{\partial^2 P_o}{\partial z^2}\right]}_{Diffusive} + \overbrace{\lambda_4\frac{\partial P_o}{\partial x}+\lambda_3\frac{\partial P_o}{\partial y}+\lambda_2\frac{\partial P_o}{\partial z}}^{Convective} + \underbrace{\lambda_1}_{Accelerative} \tag{12.0}$$

The coefficients in Eqn. (12.0) are;

λ_1 = Accelerative term , λ_2, λ_3, λ_4 = Convective term I,II,III respectively

λ_5, λ_6, λ_7 = Diffusive term I,II,III respectively

$$A_x = \Delta y \times \Delta z \qquad A_y = \Delta x \times \Delta z;\ A_z = Ay.\sqrt{2} \qquad \Delta x = \Delta y \neq \Delta z;\ A_x = A_y \approx A_z$$

By applying *Laplacian's* operator the developed 3-D, multiphase numerical model becomes;

$$A_c\left[\left(M_o\right)\left(1+B_{g/o}R_{so}\right)+\left(M_w\right)\left(1+B_{g/w}R_{Sw}\right)+\left(M_g\right)\right]\nabla^2 P_o +$$
$$A_c\left[B_o\nabla\left(\frac{M_o}{B_o}\right)+B_w\nabla\left(\frac{M_w}{B_w}\right)+B_g\left\{\nabla\left(\frac{M_g}{B_g}\right)+\left(\frac{M_w}{B_w}\right)\nabla R_{sw}+\left(\frac{M_o}{B_o}\right)\nabla R_{so}\right\}\right]\nabla P_o +$$
$$A_c(gh)\left[\left(M_o\nabla^2\rho_o\right)\left(1+B_{g/o}R_{So}\right)+\left(M_w\nabla^2\rho_w\right)\left(1+B_{g/w}R_{Sw}\right)+\left(M_g\nabla^2\rho_g\right)\right]+$$
$$\left(B_g\nabla\left(\frac{M_g}{B_g}\right)\nabla\ P_{cg}-B_w\nabla\left(\frac{M_w}{B_w}\right)\nabla\ P_{cw}\right)+\left[\left(M_g\right)\nabla^2 P_{cg}-\left(M_w\right)\nabla^2 P_{cw}\right]+$$
$$\left(M_w B_{g/w}\right)\left(\nabla R_{sw}\right)\nabla P_{cg}+\left(M_o B_{g/o}\right)\left(\nabla R_{so}\right)\nabla P_{cg}+\left[\Sigma\left(B_i q_i\right)\right]$$
$$=$$
$$V_R\phi\left[\left\{S_o\left(B_{g/o}\right)\left(\frac{\partial R_{so}}{\partial P_o}\right)+S_w\left(B_{g/w}\right)\left(\frac{\partial R_{sw}}{\partial P_o}\right)\right\}-\left\{\begin{matrix}\left(\frac{S_o}{B_o}\right)\frac{\partial B_o}{\partial P_o}+\left(\frac{S_w}{B_w}\right)\frac{\partial B_w}{\partial P_o}\\+\left(\frac{S_g}{B_g}\right)\frac{\partial B_g}{\partial P_o}\end{matrix}\right\}\right]\frac{\partial P_o}{\partial t} \quad (13.0)$$

Where subscripts 'i' represents oil, water and gas phase successively.

Application of the derived model

At the initial state, only the production well (cell) has Vorticity strength, $\Delta\Gamma$, i.e.

$\Delta\Gamma = A\times\Delta P_o = A\times C\,\Delta t,$

where A = Area of the well

Accelerative step

$$\alpha_1 = \frac{\partial P_o}{\partial t} \quad (14.0)$$

From Equation (20.0) pressure Vorticity is given by

$$\Delta P_o = C_9\ \Delta t \quad (15.0)$$

Vorticity strength = Pressure vorticity × Area, where area is the area of each cell i.e. $\Delta x\times\Delta y,$ except for the production cell in which the area is that of the well, i.e, $2\pi r\,h$. [9]

Let, h ≈ 1 for a 3-D analysis, hence Vorticity strength, Γ is given as

$$\Delta\Gamma = A\times\Delta P_o = A\times C_9\ \Delta t \quad (16.0)$$

Diffusive Step

For the diffusive step only the diffusive term in models are considered i.e.

$$\beta\left[\frac{\partial^2 P_o}{\partial x^2}+\frac{\partial^2 P_o}{\partial y^2}+\frac{\partial^2 P_o}{\partial z^2}\right]=\frac{\partial P_o}{\partial t} \quad (17.0)$$

The solution of this is given as (by analogy to that proposed by Chorin, 1967),

$$\Delta P_o = \frac{\Delta\Gamma}{4\pi\upsilon t}\exp\left(\frac{-r^2}{4\upsilon t}\right) \quad (18.0)$$

r = distance of contributing adjacent cell to a cell in cell to cell diffusion. υ = Constants, and t = time step.

Convective Step

The new vorticity strength for each cell is given by,

$$\Delta\Gamma = \frac{\Delta P_o\,4\pi\upsilon t}{\exp\left(\frac{-r^2}{4\upsilon t}\right)} \quad (19.0)$$

$$r = \sqrt{\left((u \times \Delta t)^2 + (v \times \Delta t)^2 \right)} = \Delta t \sqrt{\left((u)^2 + (v)^2 \right)} \quad (20.0)$$

The updated vorticity strength, $\Delta\Gamma^i$, is now used to calculate the new / updated pressure vorticity for each cell.

$$\Delta P_o^{\,i} = \frac{\Delta\Gamma^i}{A} \quad (21.0)$$

Where, $\Delta P_o^{\,i}$ is the updated pressure vorticity, and this was calculated for each cell.

The simulation flowchart to evaluate coefficients is as given in Fig.1 while the new pressure vorticity is added to the initial pressure estimate of the cells to give the new pressure at that time step as shown in Table 1.

III. FIGURES AND TABLES

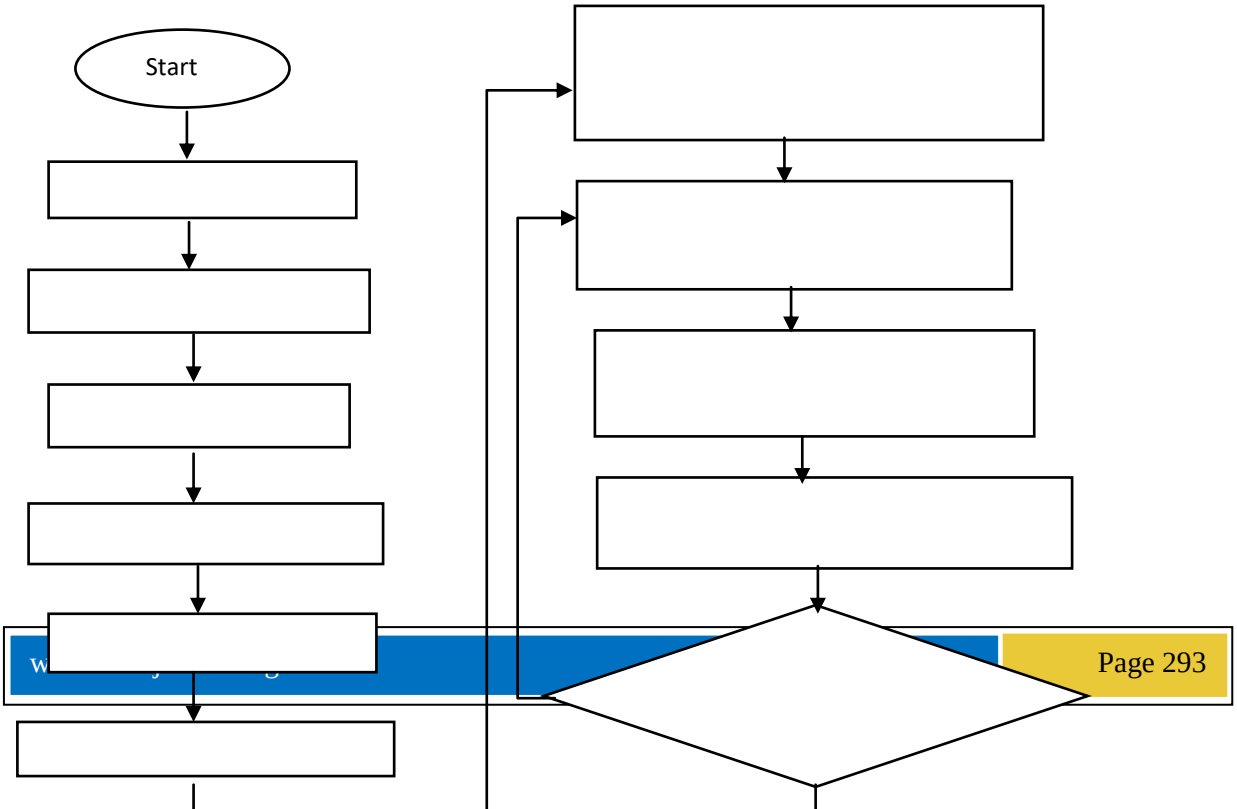

Fig.1 Flowchart for coefficients evaluation and estimation of reservoir conditions.

Table 1. Summary of hypothetical cellular pressure history in reservoir

Cell 1				
Run	**time t**	**Pressure of Oil (estimate)**	**Pressure of water (Evaluated)**	**Pressure of gas Evaluated)**
1	**0**	$(P_o)_1$	$(P_w)_1$	$(P_g)_1$
2	Δ t	$(P_o)_2 = \Delta (P_o)_1 + (P_o)_1$	$(P_w)_2$	$(P_g)2$
…	…	…	…	…
N	**Δt**	$(P_o)_n = \Delta (P_o)_{(n-1)} + (P_o)_{(n-1)}$	$(P_w)_n$	$(P_g)_n$

Table 2. Hypothetical summary of cellular saturation history for cell 1 in the 'n x n' grids.

Cell 1							
Run	**Time, t**	**Pressure**	**Formation factor (tables)**	**Saturation of oil (estimate)**	**Formation factor (tables)**	**Saturation of water (estimated)**	**Saturation of gas (evaluated)**
1	**0**	**(Po)1**	**(Bo)1**	**(So)1**	**(Bw)1**	**(Sw)1**	**(Sg)1**
2	**Δ*t***	**(Po)2**	**(Bo)2**	**(So)2**	**(Bw)2**	**(Sw)2**	**(Sg)2**
4	**Δ*t*+3Δ*t***	**(Po)4**	**(Bo)4**	**(So)4**	**(Bw)4**	**(Sw)4**	**(Sg)4**
…	…	…	…	…	…	…	…
n	**Δ*t*+(n-1)Δ*t***	**(Po)n**	**(Bo)n**	**(So)n**	**(Bw)n**	**(Sw)n**	**(Sg)n**

Saturations update of reservoir oil

$$\left(\frac{S_o}{B_o}\right)_{t=\Delta t} = \left(\frac{S_o}{B_o}\right)_{t=0} + \frac{q_o \Delta t}{V_R \phi} + \frac{A\Delta t}{V_R \phi}\left[\begin{array}{l}\left(\frac{k_o}{\mu_o B_o}\right)\left(\frac{\partial^2 P_o}{\partial x^2}+\frac{\partial^2 P_o}{\partial y^2}+\frac{\partial^2 P_o}{\partial z^2}\right) \\ +\frac{\partial P_o}{\partial x}\frac{\partial}{\partial x}\left(\frac{k_o}{\mu_o B_o}\right)+\frac{\partial P_o}{\partial y}\frac{\partial}{\partial y}\left(\frac{k_o}{\mu_o B_o}\right) \\ +\frac{\partial P_o}{\partial z}\frac{\partial}{\partial z}\left(\frac{k_o}{\mu_o B_o}\right)\end{array}\right] \quad . (22.0)$$

Where, $\left(\frac{S_o}{B_o}\right)_{t=\Delta t}$ gives the new oil saturation, (S_o) after time, Δt. This implies that, in order to evaluate the new oil saturation (S_o), the new formation factor $(B_o)_{t=\Delta t}$ needs to be known and this is a function of the new

pressure i.e. $(P_o)_{t=\Delta t} = (P_o)_{t=0} + (\Delta P_o)_{t=\Delta t}$. The new pressure, $(P_o)_{t=\Delta t}$, was used to evaluate the value of the new $(B_o)_{t=\Delta t}$ from the table relations between pressure and formation factor. With $(B_o)_{t=\Delta t}$ the new oil saturation (S_o) was evaluated by

$$(S_o)_{t=\Delta t} = \left(\frac{S_o}{B_o}\right)_{t=\Delta t} \times (B_o)_{t=\Delta t} \quad (23.0)$$

Saturations update of reservoir water

$$\left(\frac{S_w}{B_w}\right)_{t=\Delta t} = \left(\frac{S_w}{B_w}\right)_{t=0} + \frac{q_w \Delta t}{V_R \phi} + \frac{A\Delta t}{V_R \phi}\left[\begin{array}{l}\left(\frac{k_w}{\mu_w B_w}\right)\left(\frac{\partial^2 P_w}{\partial x^2} + \frac{\partial^2 P_w}{\partial y^2} + \frac{\partial^2 P_w}{\partial z^2}\right) \\ + \frac{\partial^2 P_w}{\partial x}\frac{\partial}{\partial x}\left(\frac{k_w}{\mu_w B_w}\right) + \frac{\partial P_w}{\partial y}\frac{\partial}{\partial y}\left(\frac{k_w}{\mu_w B_w}\right) \\ + \frac{\partial^2 P_w}{\partial z}\frac{\partial}{\partial z}\left(\frac{k_w}{\mu_w B_w}\right)\end{array}\right]$$

Using the new water pressure $(P_w)_{t=\Delta t}$, the new formation factor $(B_w)_{t=\Delta t}$ was evaluated from the water pressure (P_w) and formation factor, (B_w) table relations. With the new $(B_w)_{t=\Delta t}$, the new (S_w) is;

$$(S_w)_{t=\Delta t} = \left(\frac{S_w}{B_w}\right)_{t=\Delta t} \times (B_w)_{t=\Delta t} \quad (24.0)$$

Saturation update of Reservoir gas

Finally the gas saturations (S_g) were evaluated using Equation. (31.0)

$$S_o + S_w + S_g = 1 \quad (25.0)$$

The new gas saturation (S_g) was evaluated using,

$$\left(S_g\right)_{t=\Delta t} = 1 - \left(\left(S_o\right)_{t=\Delta t} - \left(S_w\right)_{t=\Delta t}\right) \quad (26.0)$$

IV. RESULTS AND DISCUSSION

As Crude oil is continually withdrawn, the reservoir equilibrium is disturbed and the associated natural gas within the crude oil stream is dislodged as shown in Figs. 2, 3, 5, 8 and hence, sudden evolution of natural gas which may not be visibly captured until the natural gas reaches its bobble pressure as occurred after the sixth day of continuous withdrawal. Since withdrawal just commenced, the gas saturation within the layer are so little and will be deposited at the topmost layer of the reservoir. The blue, red and green colour denotes indicators of reservoir water, crude oil and reservoir gas respectively. The yellow colour indicates the interface of oil and gas while the pink colour is an interface between water and oil. It was also obvious that the higher the withdrawal flow rate, the faster the draining of the Reservoir and hence, the evolution of gas and of course, the quicker the reservoir depletion. The condition of the reservoir at this stage may necessitate any enhanced oil recovery (EOR) method. Numerical outputs were shown in Tables 3 and 4. The saturation values of oil and dislodged natural gasat the withdrawal layer i.e. layer 5 within the reservoir for different time interval were given. Figures 9 and 10 gives the variation of the oil withdrawal with time.

Table 3. Results / Outputs for Reservoir Simulation process with 16 Cellular Vortex layers and 1 Vortex image at withdrawal rate of 0.46x10^{-15} m^3/s of crude oil per day

Simulation Time Step in seconds = 86400. Day under investigation = 6

Total Number of Nodes = 1936. Vortex Layer = 5

Oil saturation distribution / history

1.00000	1.000000	1.000000	1.00000	1.00000	1.000000	1.000000	1.00000	1.00000	1.000000	1.00000
1.00000	1.000000	1.000000	1.00000	1.00000	1.000000	1.000000	1.00000	1.00000	1.000000	1.00000
1.00000	.999999	.999999	.999999	.999998	.999997	.999996	.999995	.999992	.999991	.999986
.999984	.999977	.999974	.999962	.999959	.999939	.999938	.999907	.999908	.999860	.999866
.999795	.999810	.999706	.999735	.999587	.999637	.999430	.999511	.999225	.999349	.998961

.999145 .998627 .998890 .998206 .998575 .997683 .998188 .997037 .997717 .996247 .997148
.995289 .996465 .994133 .995652 .992750 .994688 .991104 .993552 .989157 .992220 .986867
.990666 .984185 .988862 .981061 .986776 .977438 .984374 .973254 .981619 .968441 .978470
.962925 .974884 .956627 .970813 .949461 .966207 .941332 .961010 .932141 .955164 .921778
.948604 .910127 .941264 .897063 .933070 .882451 .923944 .866149 .913804 .848003 .902562
.827850 .890124 .805516 .876389 .780815 .861253 .753552 .844603 .723517 .826320 1.000000

Gas saturation distribution / history

.000000 .000000 .000000 .000000 .000000 .000000 .000000 .000000 .000000 .000000 .000000
.000000 .000000 .000000 .000000 .000000 .000000 .000000 .000000 .000000 .000000 .000000
.000000 .000001 .000001 .000001 .000002 .000003 .000004 .000005 .000008 .000009 .000014
.000016 .000023 .000026 .000038 .000041 .000061 .000062 .000093 .000092 .000140 .000134
.000205 .000190 .000294 .000265 .000413 .000363 .000570 .000489 .000775 .000651 .001039
.000855 .001373 .001110 .001794 .001425 .002317 .001812 .002963 .002283 .003753 .002852
.004711 .003535 .005867 .004348 .007250 .005312 .008896 .006448 .010843 .007780 .013133
.009334 .015815 .011138 .018939 .013224 .022562 .015626 .026746 .018381 .031559 .021530
.037075 .025116 .043373 .029187 .050539 .033793 .058668 .038990 .067859 .044836 .078222
.051396 .089873 .058736 .102937 .066930 .117549 .076056 .133851 .086196 .151997 .097438
.172150 .109876 .194484 .123611 .219185 .138747 .246448 .155397 .276483 .173680 .000000

Table 4. Results / Outputs for Reservoir Simulation process with 16 Cellular Vortex layers and 1 Vortex image at withdrawal rate of 1.84×10^{-15} m^3/s of crude oil per day

Simulation Time Step in seconds = 86400. Day under investigation = 6
Total Number of Nodes = 1936. Vortex Layer = 5

Oil saturation distribution / history

1.00000 1.000000 1.000000 1.00000 1.00000 1.000000 1.000000 1.00000 1.00000 1.000000 1.00000
1.00000 1.000000 1.000000 1.00000 1.00000 1.000000 1.000000 1.00000 .999999 .999999 .999999
.999998 .999997 .999996 .999994 .999992 .999989 .999983 .999979 .999969 .999963 .999945
.999937 .999907 .999897 .999847 .999838 .999758 .999753 .999627 .999632 .999440 .999466
.999180 .999242 .998826 .998943 .998349 .998551 .997720 .998045 .996901 .997398 .995848
.996583 .994510 .995564 .992828 .994303 .990735 .992756 .988153 .990873 .984995 .988599
.981161 .985871 .976541 .982619 .971009 .978764 .964428 .974222 .956642 .968898 .947482
.962686 .936759 .955473 .924265 .947133 .909776 .937529 .893041 .926514 .873792 .913925
.851734 .899587 .826547 .883311 .797886 .864894 .765377 .844116 .728617 .820739 .687171
.794511 .640574 .765160 .588325 .732396 .529887 .695907 .464687 .655362 .392112 .610409
.311509 .560673 .222183 .505754 .123392 .445229 .014352 .378649 .000000 .305539 1.00000

Gas saturation distribution / history

.000000 .000000 .000000 .000000 .000000 .000000 .000000 .000000 .000000 .000000 .000000
.000000 .000000 .000000 .000000 .000000 .000000 .000000 .000000 .000001 .000001 .000001
.000002 .000003 .000004 .000006 .000008 .000011 .000017 .000021 .000031 .000037 .000055
.000063 .000093 .000103 .000153 .000162 .000242 .000247 .000373 .000368 .000560 .000534
.000820 .000758 .001174 .001057 .001651 .001449 .002280 .001955 .003099 .002602 .004152
.003417 .005490 .004436 .007172 .005697 .009265 .007244 .011847 .009127 .015005 .011401
.018839 .014129 .023459 .017381 .028991 .021236 .035572 .025778 .043358 .031102 .052518
.037314 .063241 .044527 .075735 .052867 .090224 .062471 .106959 .073486 .126208 .086075
.148266 .100413 .173453 .116689 .202114 .135106 .234623 .155884 .271383 .179261 .312829
.205489 .359426 .234840 .411675 .267604 .470113 .304093 .535313 .344638 .607888 .389591
.688491 .439327 .777817 .494246 .876608 .554771 .985648 .621351 1.00000 .694461 .000000

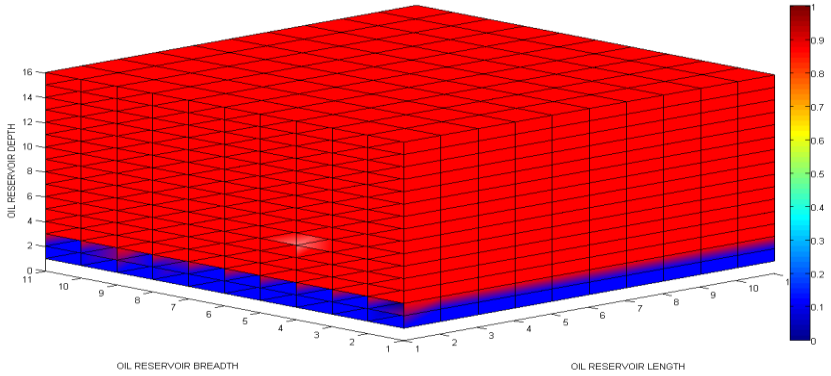

Fig. 2. Oil reservoir conditions before withdrawal i.e. initial saturation condition of the reservoir

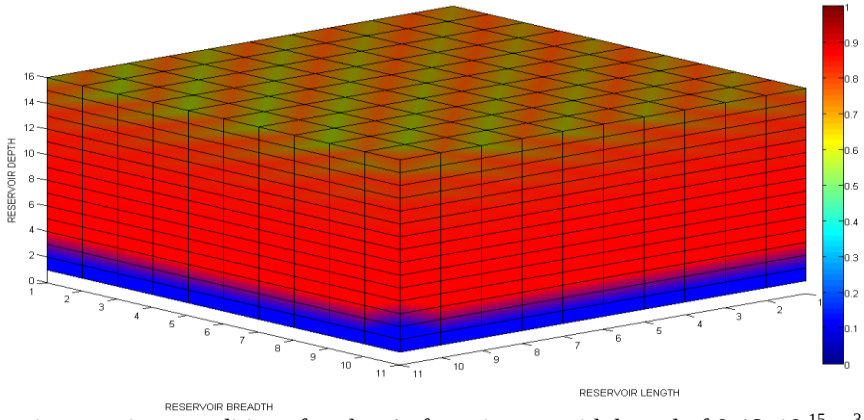

Fig. 3. Reservoir saturations condition after day 4 of continuous withdrawal of $0.46x10^{-15}$ m^3/s (250 bb/d)

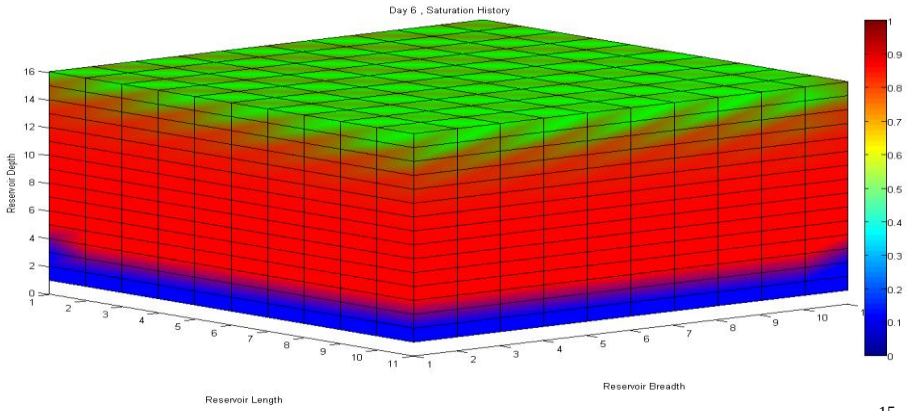

Fig. 4. Reservoir saturations condition after day 6 of continuous withdrawal of $0.46x10^{-15}$ m^3/s (250 bb/d)

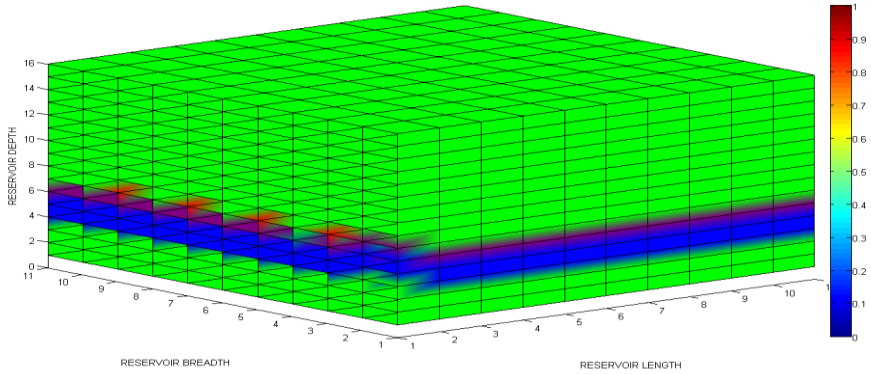

Fig. 5. Reservoir saturations condition after day 365 of continuous withdrawal of $0.46x10^{-15}$ m^3/s (250 bb/d)

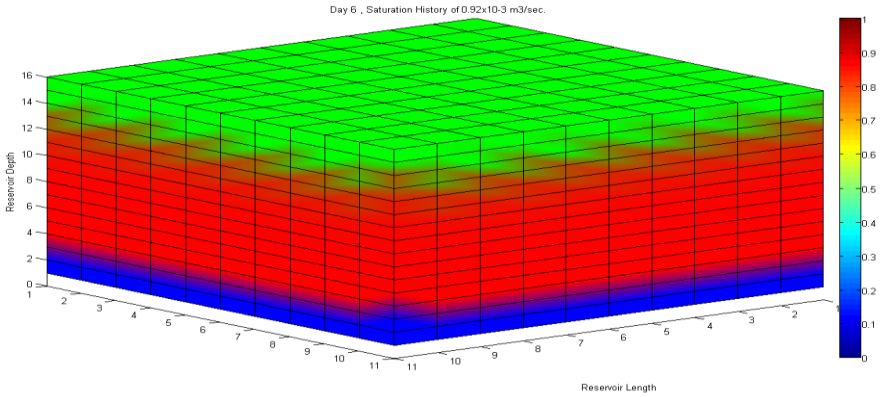

Fig. 6. Reservoir saturations condition after day 6 of continuous withdrawal of $0.92x10^{-15}$ m^3/s (500 bb/d)

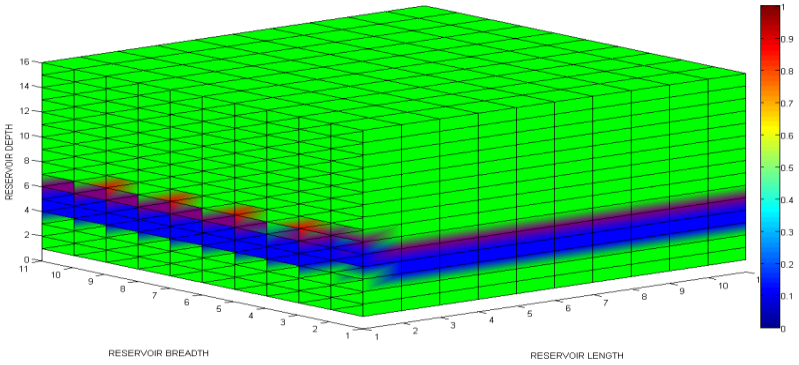

Fig. 7. Reservoir saturations condition after day 365 of continuous withdrawal of $0.92x10^{-15}$ m^3/s (500 bb/d)

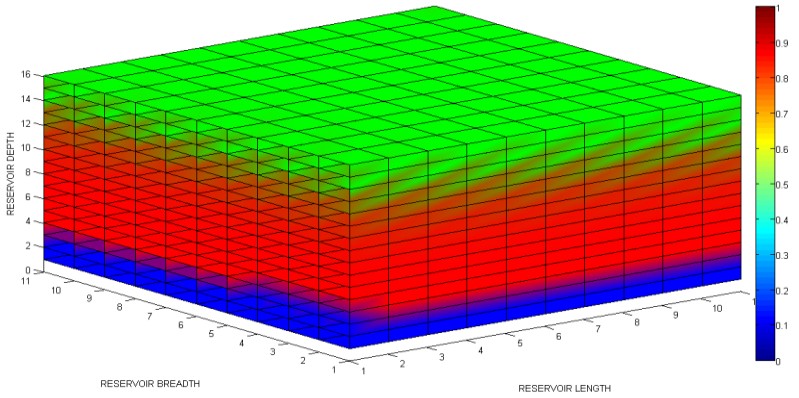

Fig. 8. Reservoir saturations condition after day 4 of continuous withdrawal of $1.84x10^{-15}$ m^3/s (1000 bb/d)

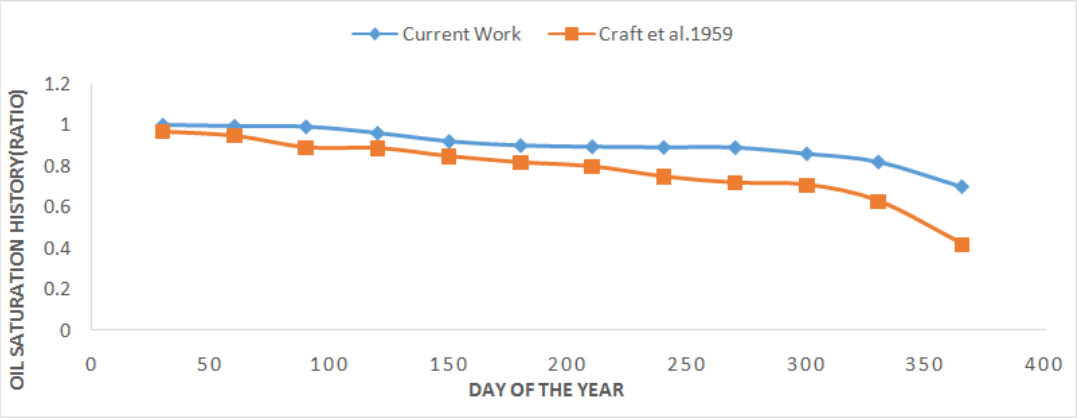

Fig. 9. Oil saturations history during continuous withdrawal for 365 days

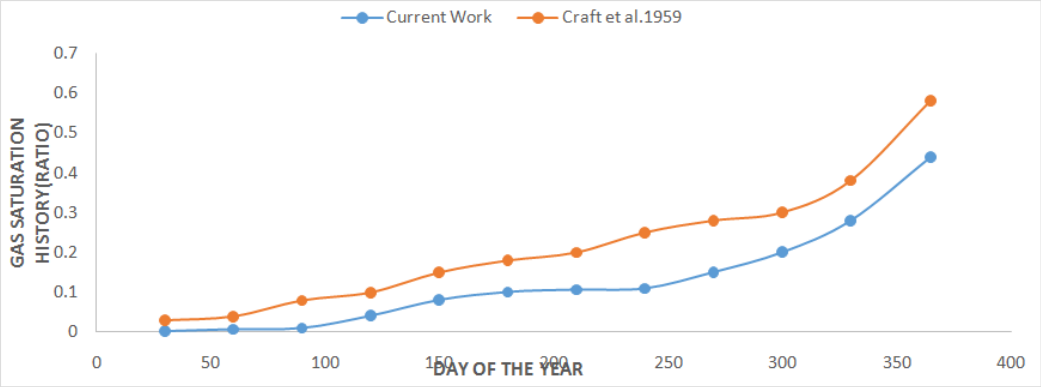

Fig. 10. Gas saturations history during continuous withdrawal for 365 days

V. CONCLUSION AND RECOMMENDATION

The generated 3-D numerical models have shown that cellular vortex method is another viable numerical method to investigate flow of fluid in fractured subsurface porous media. The crude oil is in liquid form while the dislodged natural gas is in gaseous form hence multiphase. The remarkable drop in oil saturation give rise to increase in quantity of natural gas. The cellular vortex method has proved to be efficient in terms of time of computerization, computer memory usage and also provision of output/results when the domain under investigation possess dynamic or moving tendencies. It is hereby recommended that gas capping phenomenon be investigated with this novel, ground breaking less mathematical time conscious numerical method. It is also recommended that experimental studies be carried out with a view to confirming and ascertaining the results of outputs so obtained through cellular vortex element numerical simulation.

NOMENCLATURE

κ_o	Absolute Permeability of Oil	m^2
κ_w	Absolute Permeability of Water	m^2
κ_g	Absolute Permeability of Gas	m^2
κ_r	Relative Permeability	-
κ_{ro}	Relative Permeability to oil	-
κ_{rw}	Relative Permeability to water	-
κ_{rg}	Relative Permeability to gas	-
κ_{row}	Relative Permeability to oil in oil/watersystem	-
κ_{rog}	Relative Permeability to oil in gas/oil system	-
μ	Viscosity	poise, milli-Darcy, Md
μ_o	Viscosity of Oil	poise, milli-Darcy, Md

μ_w	Viscosity of Water	poise, milli-Darcy, Md
μ_g	Viscosity of Gas	poise, milli-Darcy, Md
B	FVF (Fluid Volume Formation)	FVF,L^3/L^3,RB/STB(m^3/std m^3)
B_o	Oil Volume formation	FVF,L^3/L^3,RB/STB(m^3/std m^3)
B_g	Gas Volume formation	FVF, L^3/L^3, RB/R(m^3/ std m^3)
V	Volume	L^3, ft^3, m^3
V_R	Reservoir or Aquifer Volume	L^3, ft^3, m^3
q_o	Oil volume flow rate	L^3/t, STB/Dft^3/d, m^3/d
q_w	Water volume flow rate	L^3/t, ft^3/d, m^3/d
q_g	Gas volume flow rate	L^3/t, RB/D, ft^3/d, m^3/d
g	Acceleration due to gravity	L/t^2, m/sec^2
Φ	Potentials of fluid phase	m/Lt^2. Psi (Kpa)
Φ_o	Potentials of oil phase	m/Lt^2.psia(Kpa)
Φ_w	Potentials of water phase	m/Lt^2. psia (Kpa)
Φ_g	Potentials of gas phase	m/Lt^2. psia (Kpa)
ϕ	Porosity, fraction	-
C	Compressibility	Lt^2/m
C_o	Oil compressibility	Lt^2/m
C_w	Water compressibility	Lt^2/m
C_g	Gas compressibility	Lt^2/m
C_R	Aquifer / Reservoir rock compressibility	Lt^2/m
P_c	Phase / capillary pressure	m/Lt^2, psi(KPa)
$P_{cw} = P_{cow}$	Oil / Water capillary pressure	m/Lt^2, psi (KPa)
$P_{cg} = P_{cog}$	gas/oil capillary pressure	m/Lt^2, psi (KPa)
ρ	Fluid density	Kg/m^3,Kg/ft^3
ρ_o	Oil density	Kg/m^3,Kg/ft^3
ρ_w	Water density	Kg/m^3,Kg/ft^3
ρ_g	Gas density	Kg/m^3,Kg/ft^3
S	Saturation	-
S_o	Saturation of oil	-
S_w	Saturation of water	-
C_f	Compressibility Coefficient	-
R_s	Relative saturation	-
R_{so}	Relative saturation of oil in water- oil system	-
R_{sw}	Relative saturation(water in oil /water system)	-
$t = \Delta t$	Time of withdrawal or yield	Day or seconds
$M = k/\mu$	Mobility of fluid	-
$M_o = k_o/\mu_o$	Mobility of oil	-
$M_w = k_w/\mu_w$	Mobility of water	-
$M_g = k_g/\mu_g$	Mobility of gas	-
h_p	hydrostatic pressure	-
h_{po}	hydrostatic pressure of reservoir oil	-
h_{pw}	hydrostatic pressure of reservoir water	-
h_{pg}	hydrostatic pressure of reservoir gas	-
P_o / P_{resv}	Reservoir pressure/Reservoir oil pressure	KPa
P_{th}	Bottom hole pressure	KPa
Γ	Circulation	m^2/s
R	Cell to cell separation or distance	M

REFERENCES

[1]. Al-Yahya S. A. and Al-Anazi B. D. 2010. Reservoir monitoring and performance using Simbest II Black Oil Simulator for Middle East reservoir case study.2010. NAFTA61.Vol. 6. pp 279-283

[2]. Lie Knut-Andreas. An introduction to Reservoir simulation using MATLAB. SINTEF ICT, Department of Applied Mathematics Oslo, Norway2014 .pp 16-31

[3]. Lie Knut-Andreas and Mallison Bradly T.Mathematical Models for Oil Reservoir Simulation. 2013. pp 12-18.

[4]. Soleimani B and Nazari F. Petroleum Reservoir Simulation, Ramin Oil Field, Zagros, Iran International Journal of Modeling and Optimization, Vol. 2, No. 6(2012). pp 17-22

[5]. Stock M. J.Flow simulation with vortex elements. Independent ArtistNewton, Massachusetts, USA.2009. pp 4-6.

[6]. Ajiroba O.A. Finite difference simulation of fluid flow in an oil reservoir, Bachelor of Science Project, Department of Mechanical Engineering. University of Ibadan. (2006) xiv + 79pp

[7]. Stock M. J. 2007. Summary of Vortex Methods Literature: A living document rife with opinion II.(2007) pp 117-123

[8]. Crichlow Henry, B.Modern Reservoir Engineering - A Simulation Approach. Prentice Hall, Inc, Englewood Cliffs, New Jersey.1977 pp 34-57

[9]. Cottet, G.H. Michaux, B. Ossia, S. and Ander Linden, G.V. A comparison of spectral and vortex methods in three-dimensional incompressible flows. Journal of Computing Physics. Vol.17.(2002). Issue 2 pp 702 -712.

[10]. Craft B.C and Hawkins M.F. Applied Petroleum Reservoir Engineering. Prentice– Hall, Inc., Eaglewood Cliffs, New Jersey,1959. pp 208-315

Oyetunde Adeoye Adeaga. “Cellular Vortex Element Modeling Of Multiphase Fluid Flow In Fractured Homogenous 3-D Oil Reservoir.” American Journal of Engineering Research (AJER), vol. 6, no. 9, 2017, pp. 288–300.